



Identification of Conserved and Divergent Strigolactone Receptors in Sugarcane Reveals a Key Residue Crucial for Plant Branching Control

Anqi Hu^{1†}, Qiaoqiao Zhao^{2†}, Li Chen^{1†}, Jinping Zhao^{1,3}, Yuehua Wang¹, Kuiliang Feng¹, Ling Wu¹, Miao Xie¹, Xuemei Zhou¹, Langtao Xiao³, Zhenhua Ming^{2*}, Meng Zhang^{1*} and Ruifeng Yao^{1*}

OPEN ACCESS

Edited by:

Junxian He,
The Chinese University of Hong Kong,
China

Reviewed by:

Jian You Wang,
King Abdullah University of Science
and Technology, Saudi Arabia
Hidemitsu Nakamura,
The University of Tokyo, Japan
Hong Yu,
Institute of Genetics
and Developmental Biology, Chinese
Academy of Sciences (CAS), China

*Correspondence:

Zhenhua Ming
zhming@gxu.edu.cn
Meng Zhang
zhangmeng2019@hnu.edu.cn
Ruifeng Yao
ryao@hnu.edu.cn

[†]These authors have contributed
equally to this work

Specialty section:

This article was submitted to
Plant Physiology,
a section of the journal
Frontiers in Plant Science

Received: 25 July 2021

Accepted: 12 October 2021

Published: 11 November 2021

Citation:

Hu A, Zhao Q, Chen L, Zhao J,
Wang Y, Feng K, Wu L, Xie M,
Zhou X, Xiao L, Ming Z, Zhang M and
Yao R (2021) Identification
of Conserved and Divergent
Strigolactone Receptors in Sugarcane
Reveals a Key Residue Crucial
for Plant Branching Control.
Front. Plant Sci. 12:747160.
doi: 10.3389/fpls.2021.747160

¹ State Key Laboratory of Chemo/Biosensing and Chemometrics, Hunan Provincial Key Laboratory of Plant Functional Genomics and Developmental Regulation, College of Biology, Hunan University, Changsha, China, ² State Key Laboratory for Conservation and Utilization of Subtropical Agro-Bio Resources, Guangxi Key Laboratory for Sugarcane Biology, College of Life Science and Technology, Guangxi University, Nanning, China, ³ Hunan Province Key Laboratory of Phytohormones and Growth Development, Southern Regional Collaborative Innovation Center for Grain and Oil Crops in China, Hunan Agricultural University, Changsha, China

Strigolactones (SLs) are a class of important plant hormones mainly regulating plant architecture such as branching, which is crucial for crop yield. It is valuable to study SL signaling pathway and its physiological function in sugarcane, the most important sugar crop, for further molecular breeding. Here, two putative SL receptors SsD14a/b and the interacting F-box protein SsMAX2 were identified in *Saccharum spontaneum*. SL induced both SsD14a and SsD14b to interact with SsMAX2 in yeast. SsD14a, but not SsD14b, could bind with AtMAX2 and AtSMXL7/SsSMXL7. Overexpression of SsD14a or SsMAX2 rescued the increased branching phenotypes of *Arabidopsis thaliana d14-1* or *max2-3* mutants, respectively. Moreover, the crystal structure of N-terminal truncated SsD14a was solved, with an overall structure identical to AtD14 and OsD14 in the open state, consistent with its conserved branching suppression capacity in *Arabidopsis*. In line with the biochemical observations, SsD14b could not completely complement in *d14-1* although these two SsD14 proteins have almost identical primary sequences except for very few residues. Complement with the combination of SsD14b and SsMAX2 still failed to rescue the *d14-1 max2-3* double mutant multi-branching phenotype, indicating SsD14b–AtSMXL7 complex formation is required for regulating branching. Mutagenesis analyses revealed that residue R310 at α 10 helix of SsD14a was crucial for the binding with SsSMXL7/AtSMXL7 but not SsMAX2. The site-equivalent single-residue P304R substitution enabled SsD14b to bind with AtMAX2 and AtSMXL7/SsSMXL7 and to rescue the phenotype of *d14-1 max2-3* together with SsMAX2. Moreover, this conserved Arg residue across species including rice and *Arabidopsis* determined the activity of SL receptors through maintaining their interaction with SMXL repressors. Taken together, our work identified conserved and divergent strigolactone receptors in sugarcane core SL signaling pathway and revealed a key residue crucial for plant branching control.

Keywords: sugarcane, strigolactone, receptor, D14, MAX2, SMXL

INTRODUCTION

Strigolactones (SLs), which function as novel phytohormones in plant branching control (Gomez-Roldan et al., 2008; Umehara et al., 2008), promote the germination of root parasitic weeds (Cook et al., 1966) and regulate the symbiosis of arbuscular mycorrhizal fungi (Akiyama et al., 2005). SL biosynthesis and signaling pathway have become one of the most important and interesting research areas in recent years (Burger and Chory, 2020). Nowadays, enormous efforts have been made in studying SL signaling pathway. Several key components have been characterized, including receptor DWARF14 (D14), F-box protein MORE AXILLARY GROWTH2 (MAX2) and SUPPRESSOR OF MORE AXILLARY GROWTH2-LIKE-6 (SMXL6), SMXL7, and SMXL8 (Stirnberg et al., 2007; Umehara et al., 2008; Arite et al., 2009; Jiang et al., 2013; Stanga et al., 2013; Zhou et al., 2013). Different from other receptors, which could only sense hormone molecules, the receptor D14 have dual roles to sense and hydrolyze SL, demonstrating a brand-new function mode (Nakamura et al., 2013; Jia et al., 2014; de Saint Germain et al., 2016; Yao et al., 2016; Hu et al., 2017; Shabek et al., 2018; Marzec and Brewer, 2019; Seto et al., 2019; Lee et al., 2020). As a bifunctional receptor for SL, D14 is an α/β hydrolase with a complete catalytic triad, S97-H247-D218 (in *Arabidopsis*). The catalytic triad undergoes conformational change and hydrolyzes the four-ring complete SL molecules into two final products containing ABC-ring and D-ring, respectively (Kagiyama et al., 2013; Zhao et al., 2013; Yao et al., 2016; Hamiaux et al., 2018). During the hydrolysis of SL, D14 covalently binds to the D-ring at the catalytic center, then it associates with downstream protein MAX2/D3 to form D14-MAX2/D3 SCF E3 complex. This ubiquitin ligase complex will recruit the downstream transcription repressors SMXL6/7/8/D53, leading to the degradation of SMXLs/D53 through the 26S proteasome pathway (Hamiaux et al., 2012; Jiang et al., 2013; Yao et al., 2016; Wang et al., 2020). Thus, the downstream target genes, such as *Ideal Plant Architecture 1* (IPA1) (Song et al., 2017) which inhibited by D53, would be released to regulate plant branching. Undoubtedly, the interaction with MAX2 and SMXLs by D14 is the core to turn the transduction system on (Jiang et al., 2013; Zhou et al., 2013; Soundappan et al., 2015; Wang et al., 2015; Yao et al., 2016; Khosla et al., 2020).

As the main sugar crop, sugarcane (*Saccharum* hybrid) has great economic value (Tuma, 1987; Zhang et al., 2012). Modern commercial sugarcane varieties are derived from hybrids between *Saccharum officinarum* L. and *Saccharum spontaneum* L. The yield of *Saccharum* is usually determined by the total number of effective stems and the average single stem weight. Thus, promoting tillering and improving effective tillers are key to increase production (Aitken et al., 2008; Tena et al., 2016; Glassop et al., 2021). As an important parent, *S. spontaneum* is a representative material for sugarcane research, providing the toughness, disease resistance, and regeneration of modern sugarcane, making *S. spontaneum* an important material for SL signaling study.

Here, we studied the function of core SL signaling components from *S. spontaneum*, identified two putative SL receptors with conserved and divergent capabilities to regulate plant branching,

respectively, and revealed a key residue crucial for recruiting downstream signaling component and SL responses.

MATERIALS AND METHODS

Generation of Transgenic Plants

The modified vector pCAMBIA1300-cFlag (Yao et al., 2016) carrying the full coding sequence of *Arabidopsis thaliana* D14 (*AtD14*), *S. spontaneum* D14b (*SsD14b*), N-terminal (amino acids 1–49) truncated *S. spontaneum* D14a (*SsD14aΔN*), N-terminal (amino acids 1–44) truncated *S. spontaneum* D14b (*SsD14bΔN*) and *S. spontaneum* MAX2 (*SsMAX2*) under the control of the CaMV 35S promoter was introduced into the *Atd14-1* (Salk_057876) (Waters et al., 2012) or *Atmax2-3* (Salk_092836) (Jia et al., 2014) mutant by using the Agrobacterium-mediated floral dip method.

Similarly, we used GoldenBraid 2.0 system (Addgene¹) (Sarrion-Perdigones et al., 2013) to construct binary plant expression vectors: 35S:SsD14b-35S:SsMAX2 (P35s:SsD14b:Tnos-P35s:SsMAX2:Tnos-Pnos:NptII:Tnos), 35S:SsD14bP304R-SsMAX2 (P35s:SsD14bP304R:Tnos-P35s:SsMAX2:Tnos-Pnos:NptII:Tnos), and 35S:AtD14-35S:AtMAX2 (P35s:AtD14:Tnos-P35s:AtMAX2:Tnos-Pnos:NptII:Tnos), which were introduced into the *Atd14-1 Atmax2-1* double mutant, respectively, to generate transgenic plants. The primary rosette branching numbers were counted for 5-week-old plants, which were germinated on plates and grown in soil under a light/dark photoperiod of 16 h/8 h at 22°C.

Yeast Two-Hybrid Assays

To construct plasmids for yeast two-hybrid (Y2H) assays, the CDS of *SsD14a/b* and *SsD14a/b* truncations (*SsD14aΔN49* and *SsD14bΔN44*) were cloned into yeast expression vector pGBKT7 to generate BD-*SsD14a/b* and BD-*SsD14a/b-ΔN*, and we also constructed the mutations BD-*SsD14aR310P* and BD-*SsD14bP304R*. Similarly, we obtained BD-*OsD14* and BD-*OsD14ΔN53*. The CDS of *SsMAX2*, *AtMAX2*, and *AtSMXL7* were cloned into pGADT7 to make Gal4 DNA activation domain (AD) constructs, respectively. Y2H assays were performed using the Yeastmaker Yeast Transformation System 2 (Clontech, United States). In brief, yeast strain AH109 cells were co-transformed with specific bait and prey constructs and coating on selective growth medium SD/-Leu/-Trp for 3 days at 30°C, pick the positive constructs into liquid-selective growth medium SD/-Leu/-Trp for 36 h at 30°C, 200 rpm. Washed yeast cells three times and diluted, make sure OD₆₀₀ reached 2.5, then serial 10-fold dilutions of yeast cultures were spotted onto selective growth medium that was supplemented with 5 μM *rac*-GR24 or dimethyl sulfoxide (DMSO). All yeast transformants were grown on selective growth medium at 30°C, 4 days.

Expression and Purification of *SsD14aΔN*

The positive clones of *SsD14aΔN* (residues 1–49) proved by DNA sequencing were transformed into *Escherichia coli* strain

¹<http://www.addgene.org/browse/article/10316/>

BL21 (DE3) for protein expression. Kanamycin-resistant colonies were picked to grow in the Luria–Bertani (LB) medium (10 g/L tryptone, 10 g/L NaCl, and 5 g/L yeast extract) at 37°C until OD₆₀₀ reached 0.6–1.0. Then 0.5 mM isopropyl-beta-D-thiogalactopyranoside (IPTG) was added to induce protein expression at 16°C for 18 h. The cell pellet was resuspended in phosphate-buffered saline (PBS) buffer containing 30 mM imidazole, and homogenized by using an ultrahigh pressure cell disrupter (JNBIO, Guangzhou, China). The lysate was centrifuged at 15,000 rpm for 1 h, and soluble proteins were loaded onto the Ni-NTA column. Target proteins were eluted by the PBS buffer containing 300 mM imidazole. The eluted SsD14aΔN (residues 1–49) was further purified by SuperdexTM75 (GE Healthcare, United States) at 16°C with the buffer containing 150 mM NaCl, 2 mM MgCl₂, 20 mM Tris pH 8.0, and 10% glycerol.

Crystallization, Data Collection, and Structure Determination

Purified SsD14aΔN (residues 1–49) (roughly 10 mg/ml) were dissolved in the buffer containing 150 mM NaCl, 2 mM MgCl₂, 20 mM Tris pH 8.0, and 10% glycerol. The crystals of SsD14aΔN (residues 1–49) were obtained using the hanging-drop method by mixing 1 μl protein with equal volume of reservoir solution containing 0.01 M magnesium chloride hexahydrate, 0.05 M Tris hydrochloride pH 7.5, 5% v/v 2-Propanol at 16°C for 1 week. The data of the SsD14aΔN (residues 1–49) crystal were collected on beamline BL17U1 at Shanghai Synchrotron Radiation Facility (SSRF) and processed by XDS (20124692). The structure of SsD14aΔN (residues 1–49) was determined by molecular replacement, using the structure of OsD14ΔN (residues 1–51) (PDB ID: 3VXK) as the initial searching template. Model building and structural refinement were performed by using COOT (20383002) and PHENIX (22505256), respectively. In the final model, more than 97% residues fall in the favored region in the Ramachandran plot, and the final R_{work}/R_{free} is 0.1914/0.2275. Data collection and refinement statistics are summarized in **Table 1**. The atomic coordinates and structure factors have been deposited in the Protein Data Bank.

RESULTS

Identification of D14 Orthologs in *Saccharum spontaneum*

The SL biosynthesis and core signaling pathways have been thoroughly studied in many plant species including *Arabidopsis thaliana* and *Oryza sativa* (**Figure 1A**), but remain to be investigated in sugarcane. To identify and investigate the SL receptor(s) D14 in *S. spontaneum* (SsD14), we searched Saccharum Genome Database (SGD)² (Zhang et al., 2018) using BLAST with *Arabidopsis thaliana* D14 (AtD14) and *Oryza sativa* D14 (OsD14) as queries to obtain the predicted sequences of D14 orthologs from *S. spontaneum*. Accordingly, we found two putative D14 orthologous genes SsD14a (Sspon.001B0005800) and SsD14b (Sspon.001B0005830) in *S. spontaneum*.

²<http://sugarcane.zhangjienslab.cn>

TABLE 1 | Data collection and structure refinement statistics.

Parameters	SsD14aΔN
Data collection statistics	
Cell parameters	
<i>a</i> (Å)	48.81
<i>b</i> (Å)	88.29
<i>c</i> (Å)	118.52
α, β, and γ (°)	90, 90, and 90
Space group	<i>P</i> 2 ₁ 2 ₁ 2 ₁
Wavelength used (Å)	0.9792
Resolution (Å)	70.81–1.65 (1.74–1.65)
No. of all reflections	356,698
No. of unique reflections	580,49
Completeness (%)	93.6 (99.5)
Average <i>I</i> /σ(<i>I</i>)	12.1 (2.6)
<i>R</i> _{merge} ^a (%)	11.5 (74.4)
Refinement statistics	
No. of reflections used [σ(<i>F</i>) > 0]	110,054
<i>R</i> _{work} ^b (%)	19.14
<i>R</i> _{free} ^b (%)	22.75
RMSD bond distance (Å)	0.008
RMSD bond angle (°)	0.909
Average B-value	
Average <i>B</i> -value for protein atoms	28.69
Average <i>B</i> -value for solvent atoms	28.61
No. of atoms	
No. of protein atoms	415,0
No. of solvent atoms	357
Ramachandran plot	
Res. in favored regions (%)	97.94
Res. in outlier regions (%)	0.0

RMSD, root-mean-square deviations.

^a $R_{merge} = \sum_h \sum_l |I_{h,l} - \bar{I}_h| / \sum_h \sum_l I_{h,l}$, where, \bar{I}_h is the mean intensity of the *i* observations of symmetry-related reflections of *h*.

^b $R_{work} = \sum (|F_o(obs) - F_o(calc)|) / \sum F_o(obs)$; *R*_{free} is an *R* factor for a preselected subset (5%) of reflections that was not included in refinement. *F*_o, structure factor of protein.

^cNumbers in parentheses are corresponding values for the highest resolution shell.

The phylogenetic analysis showed that SsD14s exhibit closer relationships with OsD14 from rice, which belongs to Gramineae too (**Figure 1B**). The similarity between SsD14a and OsD14 is 84.91% at the amino sequence, and the similarity between SsD14b and OsD14 is 85.94%. Sequence alignment and structural annotation showed that SsD14a/b, AtD14, and OsD14 exhibit both considerable identities at the primary amino acid sequence level and have the same catalytic triad Ser-His-Asp (**Figure 1C**). These information implies conserved physiological functions of SsD14 proteins.

SsD14a and SsD14b Have Different Binding Properties With MAX2 and SMXLs

Similarly, we searched SGD to obtain the predicted sequences of MAX2 and SMXL7 orthologs from *S. spontaneum*. Then, we found the putative orthologous genes SsMAX2

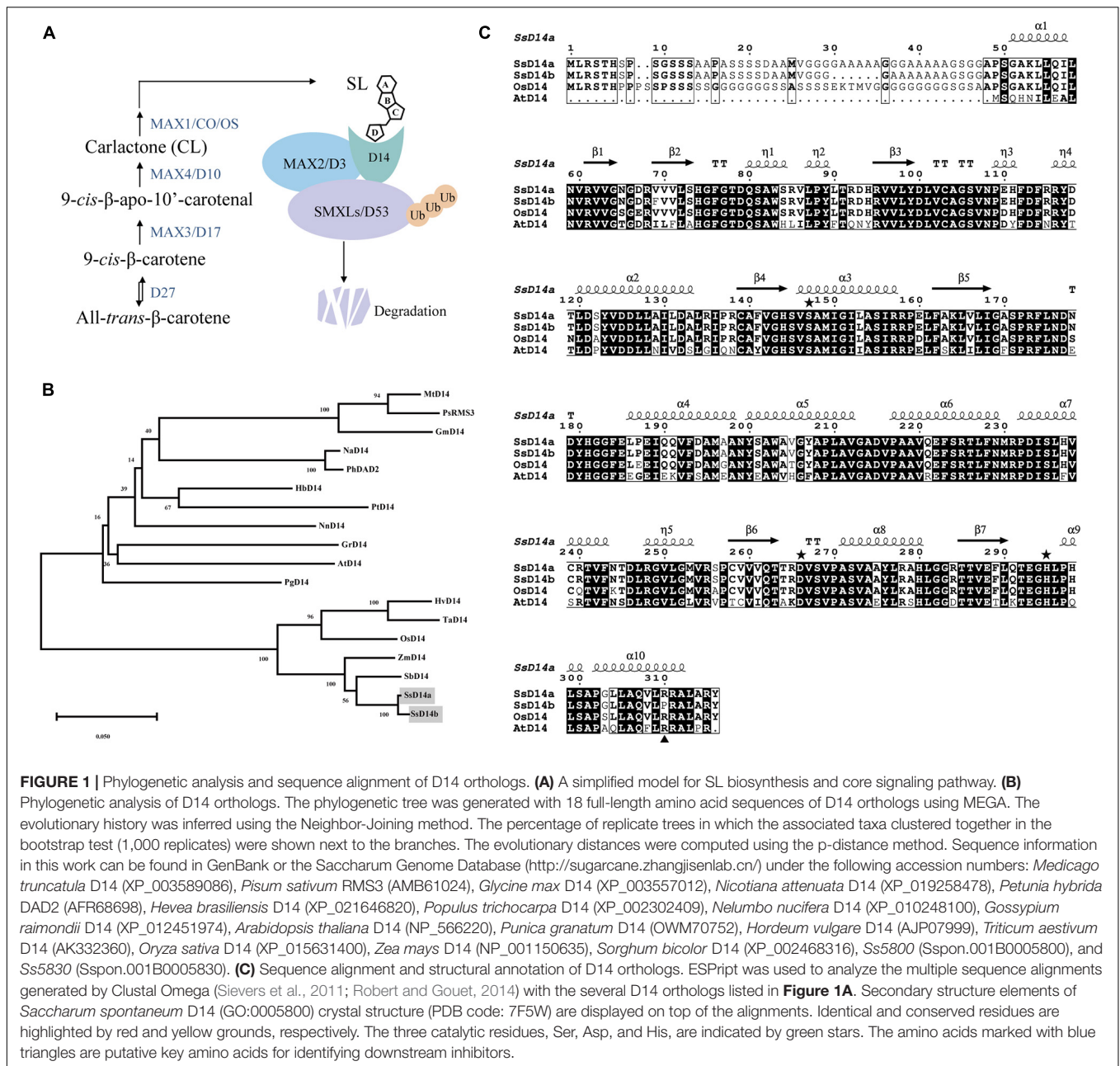


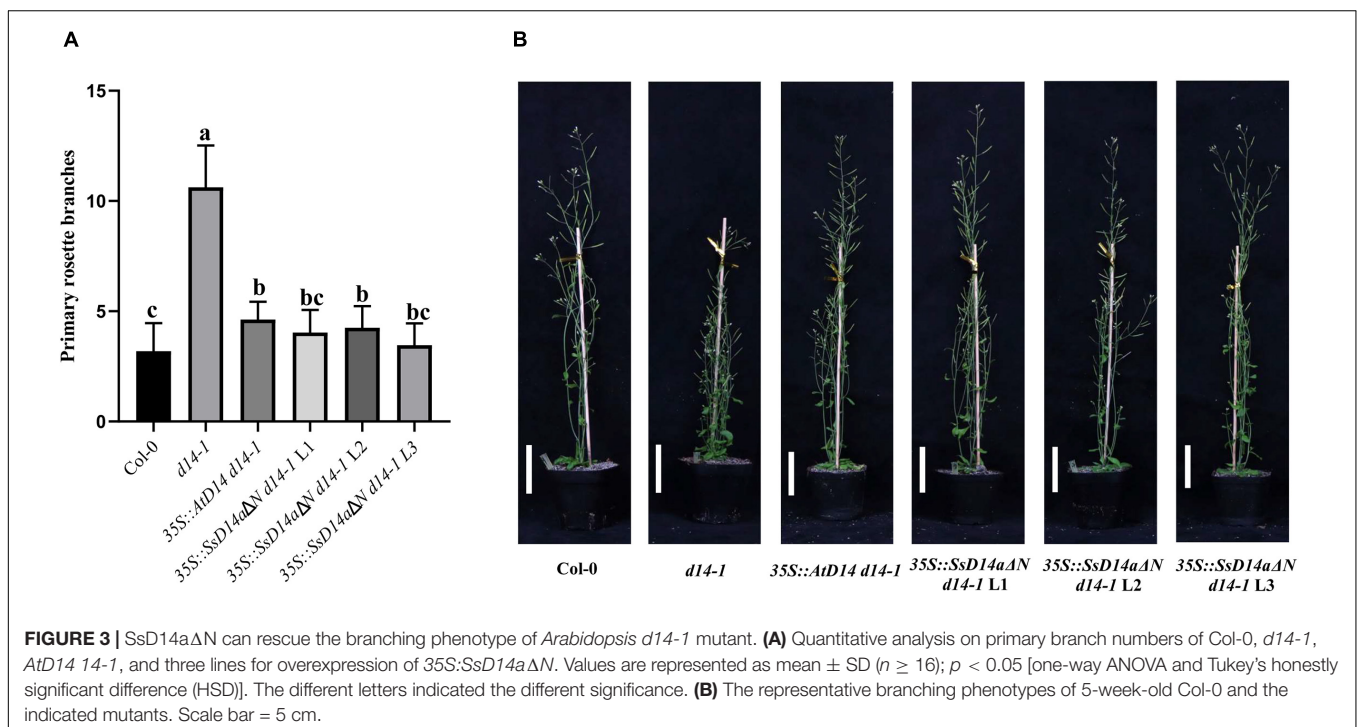
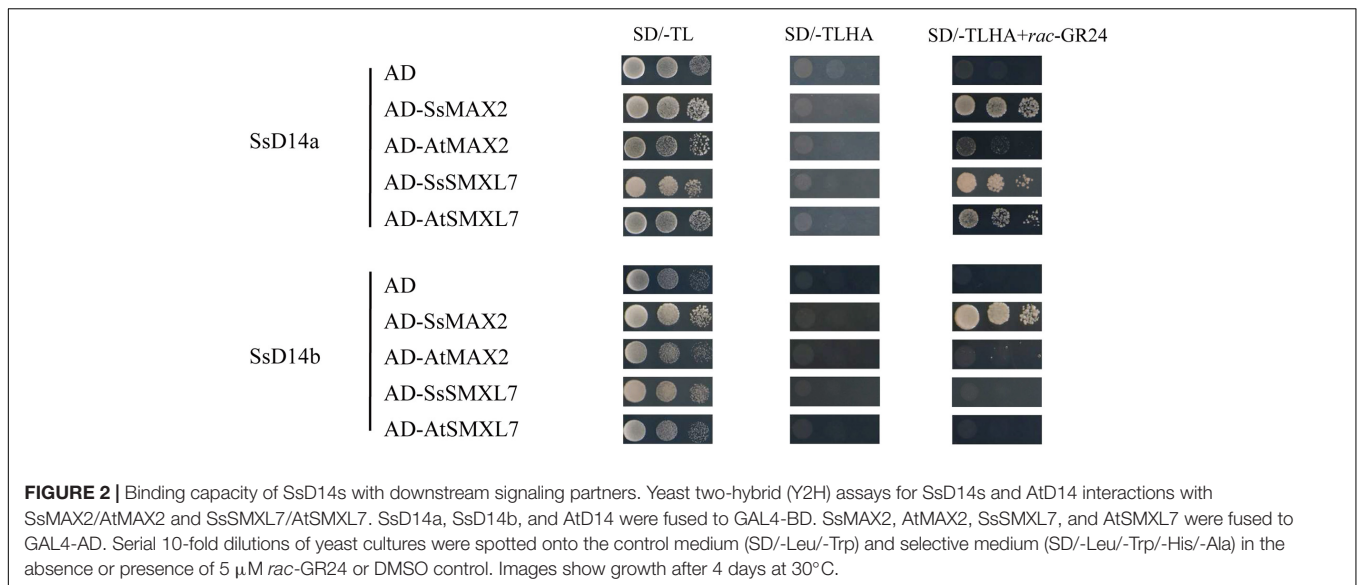
FIGURE 1 | Phylogenetic analysis and sequence alignment of D14 orthologs. **(A)** A simplified model for SL biosynthesis and core signaling pathway. **(B)** Phylogenetic analysis of D14 orthologs. The phylogenetic tree was generated with 18 full-length amino acid sequences of D14 orthologs using MEGA. The evolutionary history was inferred using the Neighbor-Joining method. The percentage of replicate trees in which the associated taxa clustered together in the bootstrap test (1,000 replicates) were shown next to the branches. The evolutionary distances were computed using the p-distance method. Sequence information in this work can be found in GenBank or the Saccharum Genome Database (<http://sugarcane.zhangjisenlab.cn/>) under the following accession numbers: *Medicago truncatula* D14 (XP_003589086), *Pisum sativum* RMS3 (AMB61024), *Glycine max* D14 (XP_003557012), *Nicotiana attenuata* D14 (XP_019258478), *Petunia hybrida* DAD2 (AFR68698), *Hevea brasiliensis* D14 (XP_021646820), *Populus trichocarpa* D14 (XP_002302409), *Nelumbo nucifera* D14 (XP_010248100), *Gossypium raimondii* D14 (XP_012451974), *Arabidopsis thaliana* D14 (NP_566220), *Punica granatum* D14 (OWM70752), *Hordeum vulgare* D14 (AJP07999), *Triticum aestivum* D14 (AK332360), *Oryza sativa* D14 (XP_015631400), *Zea mays* D14 (NP_001150635), *Sorghum bicolor* D14 (XP_002468316), Ss5800 (Sspon.001B0005800), and Ss5830 (Sspon.001B0005830). **(C)** Sequence alignment and structural annotation of D14 orthologs. ESPript was used to analyze the multiple sequence alignments generated by Clustal Omega (Sievers et al., 2011; Robert and Gouet, 2014) with the several D14 orthologs listed in Figure 1A. Secondary structure elements of *Saccharum spontaneum* D14 (GO:0005800) crystal structure (PDB code: 7F5W) are displayed on top of the alignments. Identical and conserved residues are highlighted by red and yellow grounds, respectively. The three catalytic residues, Ser, Asp, and His, are indicated by green stars. The amino acids marked with blue triangles are putative key amino acids for identifying downstream inhibitors.

(Sspon.008D0018870) and SsSMXL7 (Sspon.007A0023280). To determine the biochemical function of SsD14a and SsD14b, we used Y2H assays to examine the interaction of SsD14s proteins with SsMAX2, AtMAX2, SsSMXL7, and AtSMXL7. Surprisingly, there were significant binding ability differences between SsD14a and SsD14b. The results showed that SsD14a interacted with SsSMXL7 and AtSMXL7 and interacted with AtMAX2 slightly. However, SsD14b interacted with neither AtMAX2 nor AtSMXL7. Meanwhile, Y2H results showed a strong interaction of SsMAX2 with both SsD14a and SsD14b (Figure 2). In other words, although SsD14a and SsD14b share 97.47% similarity in amino acid sequence, they have different preferences in binding downstream signaling partners, which leading us to speculate

that the differences in interactions are attributed to some of these different residues.

SsD14aΔN, but Not SsD14b and SsD14bΔN, Can Well Rescue the Branching Phenotype of *Arabidopsis d14-1* Mutant

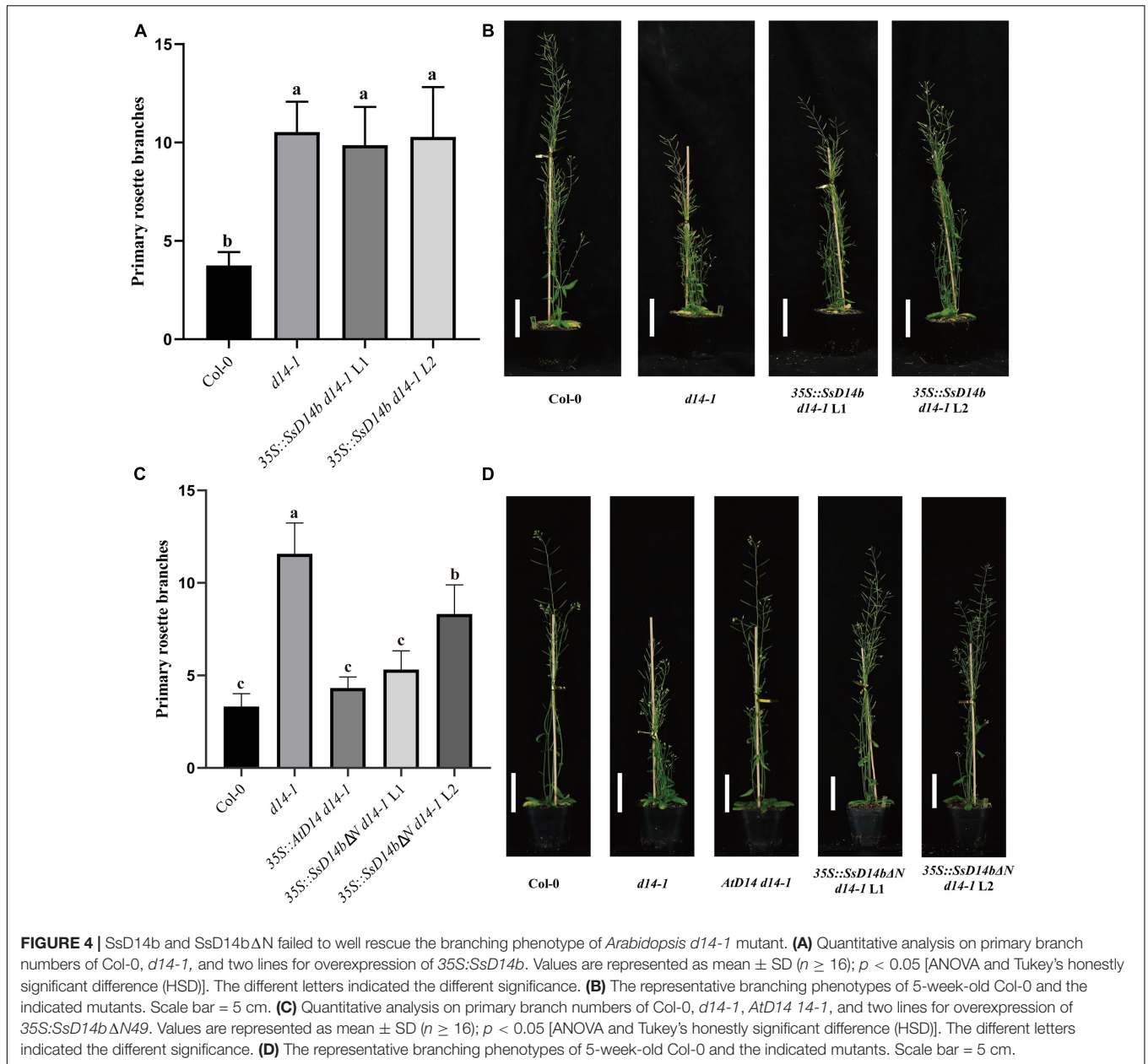
Previous reports showed that many D14 of Gramineae species contain an extra N-terminal peptides when compared to AtD14 (Yao et al., 2018). Related studies have proved that both the full-length OsD14 and the N-terminally truncated OsD14 were able to complement the multi-branching mutant *Arabidopsis d14-5*,



even the N-truncated D14 have more stronger interaction with AtMAX2 and complement *d14* mutant better than the full-length version (Yao et al., 2018). According to our results of Y2H assays, SsD14a Δ N can interact with AtMAX2 and AtSMXL7 as the full-length SsD14a did (**Supplementary Figure 1**). SsD14a Δ N was introduced to complement *Arabidopsis d14-1* mutants. We also generated the 35S::*AtD14 d14-1* plants as positive control. The results showed no significant difference between the number of primary branches between 35S::SsD14a Δ N *d14-1* and 35S::*AtD14 d14-1* (**Figures 3A,B**), which means that SsD14a Δ N was able to rescue the multi-branching phenotypes. In addition, the

leaf morphology (length/width ratio) was also recovered by SsD14a Δ N (**Supplementary Figure 2A**). Therefore, SsD14a is functionally conserved when compared with AtD14.

However, the complementation results were quite different for SsD14b. According to the Y2H results, neither N-terminal truncated SsD14b nor full-length SsD14b could interact with AtMAX2 and AtSMXL7 (**Figure 2** and **Supplementary Figure 1**). We transferred the full-length SsD14b to the *Arabidopsis d14-1* mutant and obtained 35S::SsD14b *d14-1* plants. We found that SsD14b cannot rescue the *d14-1* multi-branching phenotype (**Figure 4A**). But interestingly, we found that the height of

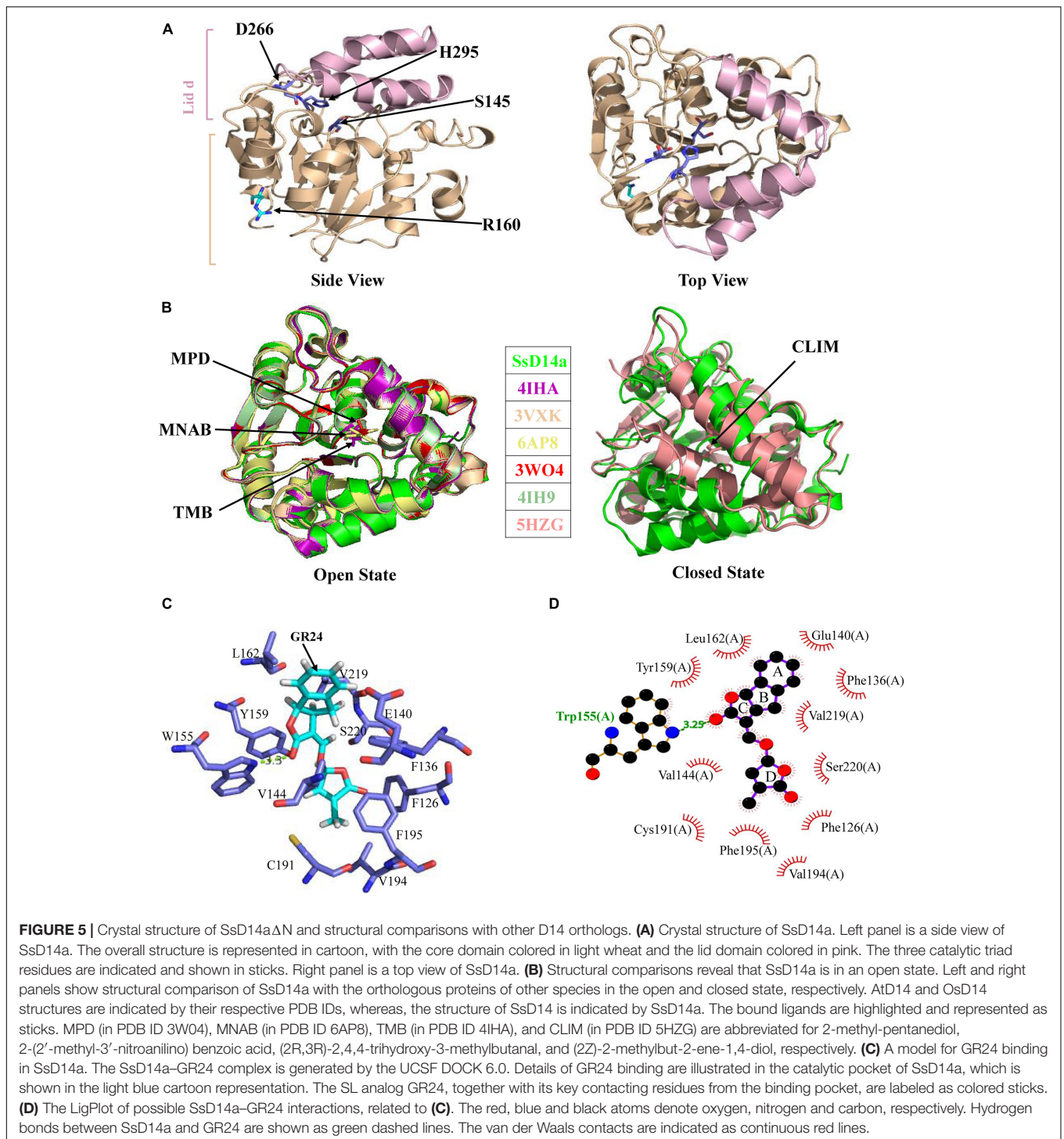


transgenic 35S::SsD14b *d14-1* seemed to have a partial restoration (Figure 4B), which will be further investigated in the future project. We found that the multi-branched phenotype of one complemented line was only partially restored in 35S::SsD14bΔN *d14-1* transgenic lines and still differed from WT, indicating that 35S::SsD14bΔN cannot fully complement *Atd14-1*. The difference between 35S::SsD14b *d14-1* and 35S::SsD14bΔN *d14-1* was that multi-branched and the leaf morphology of 35S::SsD14bΔN *d14-1* were rescued in different degrees but both not thoroughly (Figure 4 and Supplementary Figure 2B). No obvious interactions of SsD14b/SsD14bΔN with AtSMXLs were detected in our work, which is probably because that the interactions were too weak to be detected in our current Y2H system. Consistent with this, the complementation effect

of SsD14bΔN is significantly lower compared to SsD14a. Taken together, SsD14a and SsD14b may function as conserved and divergent SL receptors in sugarcane, respectively.

Crystal Structure of SsD14aΔN Possesses an Overall Architecture Identical to Other D14 Orthologs in the Open State

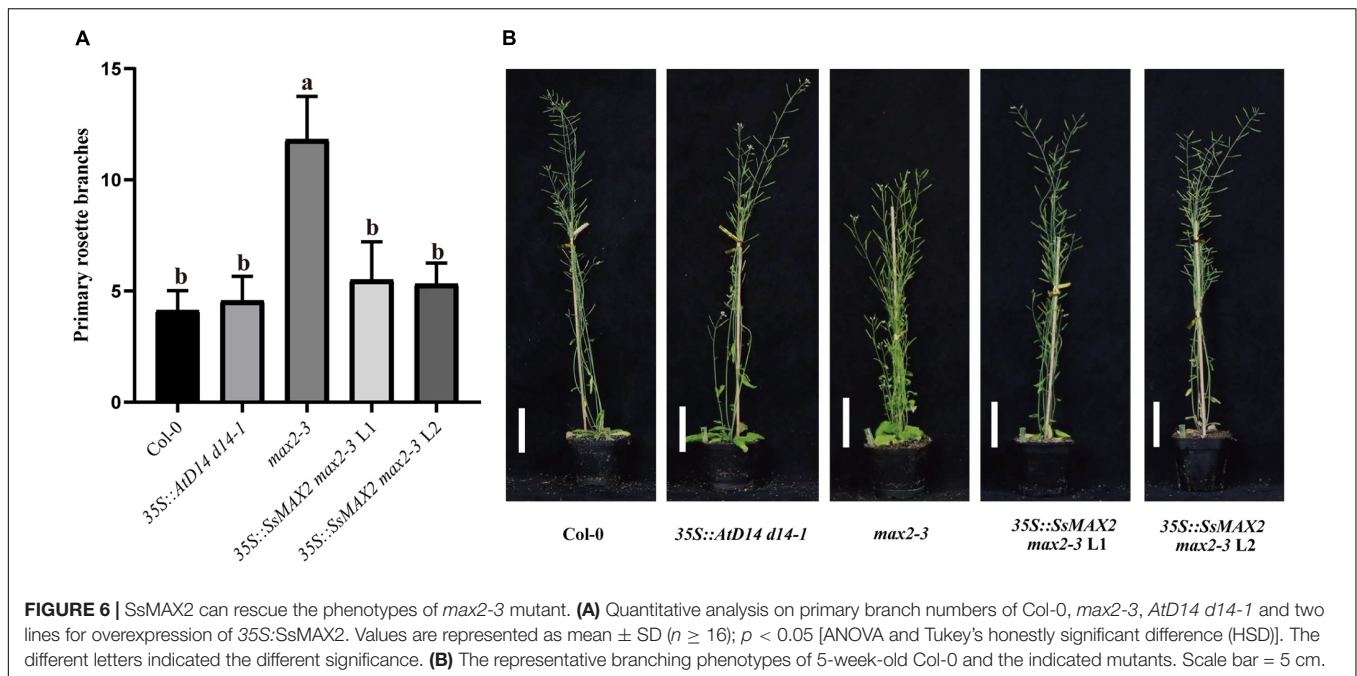
The crystal structure of SsD14aΔN was determined at a resolution of 1.65 Å (Table 1). SsD14a belongs to the α/β hydrolase superfamily, of which the structure consists of an α/β hydrolase core domain and a four-helix lid domain (αT1, αT2, αT3, and αT4) (Figure 5). The catalytic triad residues of S145,



D266, and H295, distributed on the loops following the β 4, β 6, and β 7 strands, are located at the bottom of the hydrophobic substrate-binding pocket. The rest of the core domain is made up of seven β strands (β 1- β 7) and six α helices (α 1, α 2, α 3, α 8, α 9, and α 10). R310 is located at the α 10 helix of SsD14a.

To gain insights into the conformational state of SsD14a, we performed structural comparisons between SsD14a and other

D14 orthologs from other plants. Structure comparisons revealed that the overall structure of SsD14a was identical to those from other plants in the open state (**Figure 5B**), with root-mean-square deviations (RMSD) ranging from 0.250 to 0.301 Å (**Figure 5B**). Notably, the overall structure of SsD14a in the open state was apparently larger than the closed state of AtD14-CLIM (covalently linked intermediate molecule, a hydrolysis



intermediate of SL molecule), thus these two structures cannot be well aligned, with an RMSD of 0.662 Å. Furthermore, results of docking approaches demonstrated extensive binding of GR24 by residues in the catalytic pocket of SsD14a (Figures 5C,D). In general, the structural characteristics of SsD14a are highly conserved and guarantee its branching inhibition function.

SsMAX2 Rescued the Branching Phenotype of *Arabidopsis max2-3* Mutant

To clarify the differences on SL transduction between the two SsD14 proteins, SsMAX2, another key SL signaling transduction component, was obtained and verified its function. SsMAX2 interacted with AtD14 in an SL-dependent manner with the intensity similar to AtMAX2 (Figure 2). We further investigated the physiological function of SsMAX2 proteins in *Arabidopsis*. We introduced full-length *S. spontaneum* MAX2 into the *Arabidopsis max2-3* mutant under the control of a 35S promoter. As shown in Figure 6 and Supplementary Figure 2C, 35S::SsMAX2 *max2-3* rescued the branching and leaf phenotype of *max2-3* to a level comparable with the wild-type Col-0. These genetic data indicated that SsMAX2 could inhibit axillary branching of *Arabidopsis*. Our results demonstrated that SsMAX2 can resemble AtMAX2 to play a physiological role in *Arabidopsis*.

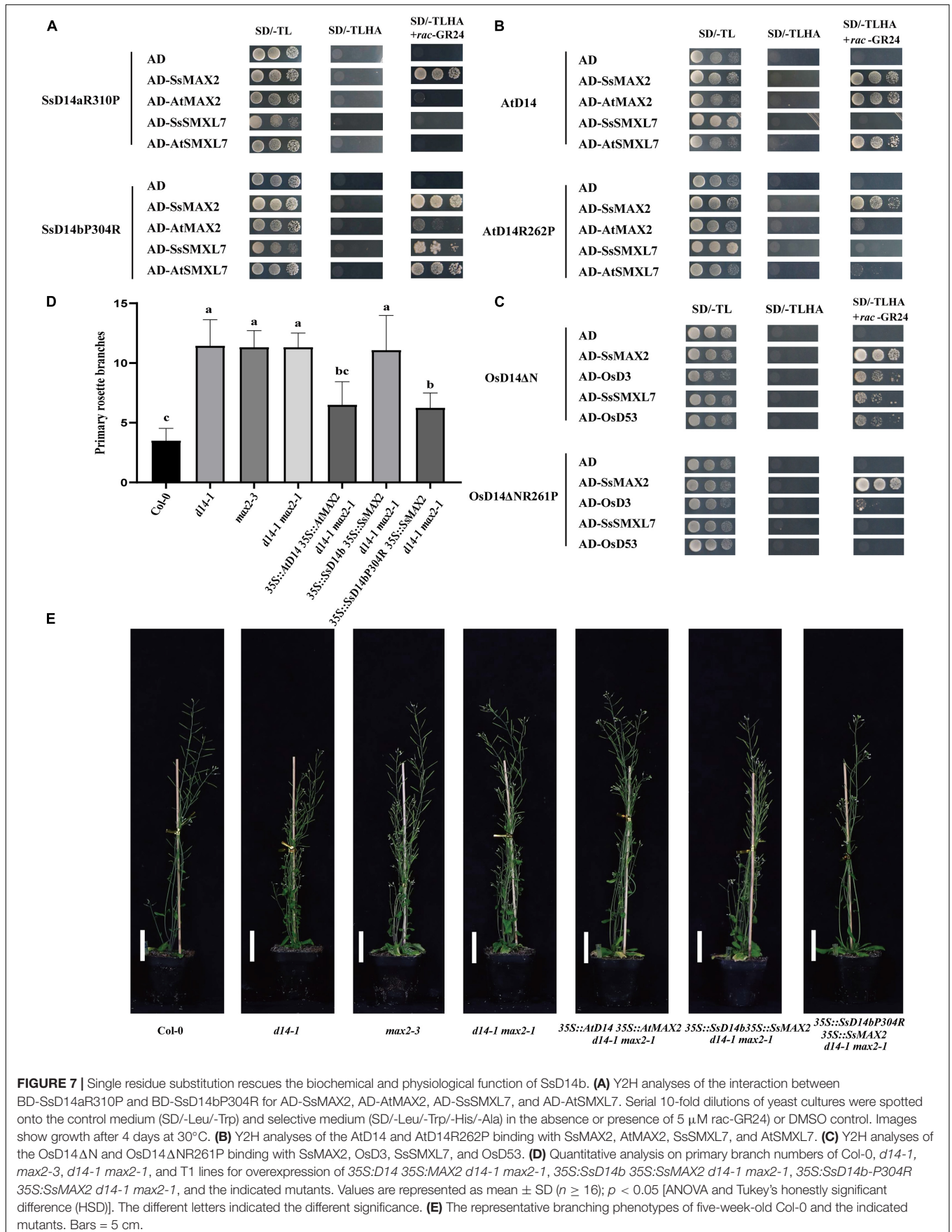
Single Residue Substitution of SsD14b Rescues the Binding Affinity With MAX2 and SMXLs

Further sequence comparison with AtD14 and OsD14 found that only SsD14b had a proline (P304) at the $\alpha 10$ helix, whereas, other D14 proteins contained an arginine (R) (Figure 1B). To further explore the mechanism underlying the differences

in protein interactions, we made point mutations to SsD14a and SsD14b to obtain BD-SsD14aR310P and BD-SsD14bP304R, respectively. We were surprised to find that the point mutation SsD14aR310P no longer interacted with SsSMXL7 and AtSMXL7 (Figure 7A), but still interacted with SsMAX2. The point mutation SsD14bP304R turn out to obviously interact with AtSMXL7. Inferring from these results, for D14, residue R (like R310 of SsD14a) at the $\alpha 10$ helix might be the key residue contributing to the association with repressor factors SMXLs.

The R262P/R312P Point Mutation Disrupts the Function of AtD14/OsD14 to Bind With Downstream Signaling Partners

To further investigate the importance and the widespread of the amino acid site of R310 (in SsD14a), we performed point mutation validation in AtD14 and OsD14. We obtained BD-AtD14R262P and BD-OsD14 Δ NR261P by site-directed mutagenesis PCR. Y2H results showed that AtD14R262P substitution largely affected the interaction with AtSMXL7 and also greatly weakened the interaction with AtMAX2 (Figure 7B). Similar observation was also found in BD-OsD14 Δ NR261P (Figure 7C). Unlike AtD14, OsD14 showed hormone-dependent interaction with SsSMXL7. We speculate that this is a result of the higher sequence similarity between rice and sugarcane, which both belong to Gramineae. Interestingly, AtD14R262P and OsD14 Δ NR261P, like wild-type proteins, still have strong hormone-dependent interactions with SsMAX2. The SsMAX2 protein can bind strongly with mutant proteins, which may have application in resolving the crystal structures of certain important D14 mutant proteins in complex with SsMAX2. In general, for AtD14 and OsD14, we further



verified the importance of this site for binding downstream signal components.

Single Residue Substitution Rescues the Physiological Function of SsD14b

In the SL signaling pathway, the D14 receptor senses SL before binding the F-box protein MAX2 to form the D14–MAX2 complex. Later, the complex would recruit and degrade the downstream repressor protein AtSMXLs through ubiquitination–proteasome pathway to regulate plant branching (Jiang et al., 2013; Zhou et al., 2013). To investigate whether SsD14bP304R has gained the capability in plant branching control, we generated and compared the transgenic *Arabidopsis* 35S:SsD14b 35S:SsMAX2 *d14-1 max2-1* and 35S:SsD14b-P304R 35S:SsMAX2 *d14-1 max2-1* by introducing full-length SsMAX2 together with SsD14b or SsD14b-P304R into the *d14-1 max2-1* double mutant. We also generated the 35:AtD14 35:AtMAX2 *d14-1 max2-1* plants as positive control. We found that 35S:SsD14b-P304R 35S:SsMAX2 *d14-1 max2-1* showed similar primary branching and leaf morphology as 35S:AtD14 35S:AtMAX2 *d14-1 max2-1* (Figures 7D,E and Supplementary Figure 2D). However, the complex of SsD14b–SsMAX2 was unable to inhibit the branching of *d14-1 max2-1* double mutant, consistent with the capability of SsD14b or SsD14b-P304R to bind AtSMXL7 (Figures 2, 7A). These results demonstrated that P304R single-residue substitution endows SsD14b with the branching inhibition function, indicating the close correlation between SL responses and receptor–repressor interaction.

DISCUSSION

Sugarcane is a raw material for sucrose and can also be used as an energy substitute for refined ethanol, which has high economic value. The effective yield of sugarcane is closely related to the effective branching and robust plant architecture. As the ancestor of modern sugarcane and possessing a complete genome database, *S. spontaneum* is an important research material. To lay a foundation for further sugarcane SL pathway studies and related molecular breeding, we turned to identify and study core SL components in *S. spontaneum*.

The SL perception by the receptor D14 initiates the SL signaling transduction pathway. At present, the function of D14 has been studied in many species, such as *Oryza sativa* (D14), *Petunia hybrida* (DAD2), and *Pisum sativum* (RMS3), certifying that D14 is highly conserved in different species (Arite et al., 2009; Hamiaux et al., 2012; de Saint Germain et al., 2016; Yao et al., 2018). Here, two D14 orthologous genes in *S. spontaneum*, SsD14a and SsD14b, were identified according to ortholog searching in *S. spontaneum* genome. SsD14a and SsD14b were extremely similar with only few residue exceptions. Additionally, evolutionary analysis showed that both SsD14s were closer to SbD14, ZmD14, and OsD14, all of which are Gramineae. However, Y2H experiments revealed that only

SsD14a could interact with AtMAX2 and AtSMXL7/SsSMXL7, whereas, SsD14b could not. Interestingly, there was no difference in the binding affinity with SsMAX2 between SsD14b and SsD14a. Transgenic *Arabidopsis* plants showed that only SsD14a could well rescue the *d14-1* mutant. Furthermore, the structure of SsD14a is identical to AtD14 and OsD14 in the open state, with RMSD ranging from 0.250 to 0.301 Å. These results indicated SsD14a functioned the same as known D14 proteins, such as AtD14, suggesting that a similar SL transduction system exists in *S. spontaneum*.

In the current model, upon perception of SL, the receptor D14 recruits MAX2 and SMXLs to initiate SL signal transduction to regulate branching. However, SsD14b has problems in binding with AtSMXL7/SsSMXL7 and AtMAX2 and is unable to transduce SL signals to inhibit branching by forming such D14–MAX2–SMXL complex. It is interesting that SsD14b, with only very few residue differences from SsD14a, cannot rescue *d14-1* mutant. Meanwhile, through further sequence comparison with AtD14, OsD14, and other reported D14 orthologs, it was found that only SsD14b contains a Proline (P) at position 304, and the rest of the D14 proteins were all Arginine (R) (Figure 1). To verify the effects of this residue site, we obtained point mutations at equivalent sites to obtain SsD14aR310P and SsD14bP304R. After Y2H verification, the point mutation of the two proteins did not affect the interaction with SsMAX2. By contrast, SsD14aR310P no longer interacted with SsSMXL7 or AtSMXL7, but SsD14bP304R interacted with SsSMXL7 and AtSMXL7, suggesting that the R310/P304 site in SsD14s did affect the interaction with the downstream repressor protein SMXLs to form functional D14–MAX2–SMXL complex.

To further verify whether the failure of SsD14b to rescue *Arabidopsis d14-1* is attributed to the loss of SMXL binding ability, we introduced SsMAX2 together with SsD14b or SsD14b-P304R into the *d14-1 max2-1* double mutant to express c D14–MAX2 complex. Our results confirmed the importance of SMXL binding by SL receptor and indicated that the assembly of complete D14–MAX2–SMXLs complex is essential for SL responses, although SsD14b–SsMAX2 complex might associate with other proteins but not SMXLs to exert certain function. Additionally, we found that SsMAX2 could bind with D14 proteins from various species much stronger than AtMAX2 and OsD3, suggesting that MAX2 proteins from different plant species may have diverse capabilities to transduce SL signal and would serve as valuable sources for structural studies on SL signaling.

Taken together, our findings shed new light on the study of strigolactone receptors and their interaction with downstream signaling partners, and may have potential application value in the molecular breeding of plant architecture.

ACCESSION NUMBER

The crystal structure of SsD14a has been deposited in the Protein Data Bank under the accession code 7F5W. *S. spontaneum* genes involved in this article can be found at the Saccharum Genome

Database (SGD: <http://sugarcane.zhangjisenlab.cn>) under the following accession numbers: *SsD14a* (Sspon.001B0005800), *SsD14b* (Sspon.001B0005830), *SsMAX2* (Sspon.008D0018870), and *SsSMXL7* (Sspon.007A0023280).

DATA AVAILABILITY STATEMENT

The datasets presented in this study can be found in online repositories. The names of the repository/repositories and accession number(s) can be found in the article/**Supplementary Material**.

AUTHOR CONTRIBUTIONS

RY, MZ, and LC conceived and designed the research. AH and MX constructed the vectors. AH performed the yeast two-hybrid assays. QZ and ZM performed the protein purification, crystallization, and structure analysis. AH, JZ, YW, KF, XZ, LW, and XZ conducted *Arabidopsis* transformation and phenotype observations. AH, QZ, LC, LX, MZ, ZM, and RY analyzed the data. AH, QZ, LC, MZ, ZM, and RY wrote the manuscript. All authors read and approved the manuscript.

REFERENCES

- Aitken, K. S., Hermann, S., Karno, K., Bonnett, G. D., McIntyre, L. C., and Jackson, P. A. (2008). Genetic control of yield related stalk traits in sugarcane. *Theor. Appl. Genet.* 117, 1191–1203. doi: 10.1007/s00122-008-0856-6
- Akiyama, K., Matsuzaki, K., and Hayashi, H. (2005). Plant sesquiterpenes induce hyphal branching in arbuscular mycorrhizal fungi. *Nature* 435, 824–827. doi: 10.1038/nature03608
- Arite, T., Umehara, M., Ishikawa, S., Hanada, A., Maekawa, M., Yamaguchi, S., et al. (2009). *d14*, a strigolactone-insensitive mutant of rice, shows an accelerated outgrowth of tillers. *Plant Cell Physiol.* 50, 1416–1424. doi: 10.1093/pcp/pcp091
- Burger, M., and Chory, J. (2020). The Many Models of Strigolactone Signaling. *Trends Plant Sci.* 25, 395–405. doi: 10.1016/j.tplants.2019.12.009
- Cook, C. E., Whichard, L. P., Turner, B., Wall, M. E., and Egle, G. H. (1966). Germination of Witchweed (*Striga lutea* Lour.): isolation and Properties of a Potent Stimulant. *Science* 154, 1189–1190. doi: 10.1126/science.154.3753.1189
- de Saint Germain, A., Clave, G., Badet-Denisot, M. A., Pillot, J. P., Cornu, D., Le Caer, J. P., et al. (2016). An histidine covalent receptor and butenolide complex mediates strigolactone perception. *Nat. Chem. Biol.* 12, 787–794. doi: 10.1038/nchembio.2147
- Glassop, D., Perroux, J., and Rae, A. (2021). Differences in sugarcane stool branching within *Saccharum spontaneum* genotypes and compared to *Saccharum officinarum* and commercial varieties. *Euphytica* 217:50. doi: 10.1007/s10681-021-02789-w
- Gomez-Roldan, V., Fervas, S., Brewer, P. B., Puech-Pages, V., Dun, E. A., Pillot, J. P., et al. (2008). Strigolactone inhibition of shoot branching. *Nature* 455, 189–194. doi: 10.1038/nature07271
- Hamiaux, C., Drummond, R. S., Janssen, B. J., Ledger, S. E., Cooney, J. M., Newcomb, R. D., et al. (2012). DAD2 is an alpha/beta hydrolase likely to be involved in the perception of the plant branching hormone, strigolactone. *Curr. Biol.* 22, 2032–2036. doi: 10.1016/j.cub.2012.08.007
- Hamiaux, C., Drummond, R. S. M., Luo, Z., Lee, H. W., Sharma, P., Janssen, B. J., et al. (2018). Inhibition of strigolactone receptors by N-phenylanthranilic acid derivatives: structural and functional insights. *J. Biol. Chem.* 293, 6530–6543. doi: 10.1074/jbc.RA117.001154
- Hu, Q., He, Y., Wang, L., Liu, S., Meng, X., Liu, G., et al. (2017). DWARF14, A Receptor Covalently Linked with the Active Form of Strigolactones, Undergoes

FUNDING

We acknowledge the funding support by the National Natural Science Foundation of China (Nos. 32070321 and 32000226), State Key Laboratory for Conservation and Utilization of Subtropical Agro-Bio resources (Nos. SKLCUSA-b201807, SKLCUSA-b201906, and SKLCUSA-b201907), China Hunan Provincial Science and Technology Department (Nos. 2019RS2019 and 2020JJ3007), and the Guangxi Natural Science Foundation (No. 2020GXNSFFA297007).

ACKNOWLEDGMENTS

We thank David C. Nelson (University of California, Riverside, CA, United States) and Ke-xuan Tang (Shanghai Jiao Tong University) for providing *Arabidopsis* mutants or vectors.

SUPPLEMENTARY MATERIAL

The Supplementary Material for this article can be found online at: <https://www.frontiersin.org/articles/10.3389/fpls.2021.747160/full#supplementary-material>

- Strigolactone-Dependent Degradation in Rice. *Front. Plant Sci.* 8:1935. doi: 10.3389/fpls.2017.01935
- Jia, K. P., Luo, Q., He, S. B., Lu, X. D., and Yang, H. Q. (2014). Strigolactone-regulated hypocotyl elongation is dependent on cryptochrome and phytochrome signaling pathways in *Arabidopsis*. *Mol. Plant* 7, 528–540. doi: 10.1093/mp/sst093
- Jiang, L., Liu, X., Xiong, G., Liu, H., Chen, F., Wang, L., et al. (2013). DWARF 53 acts as a repressor of strigolactone signalling in rice. *Nature* 504, 401–405. doi: 10.1038/nature12870
- Kagiya, M., Hirano, Y., Mori, T., Kim, S. Y., Kyozuka, J., Seto, Y., et al. (2013). Structures of D14 and D14L in the strigolactone and karrikin signaling pathways. *Genes Cells* 18, 147–160. doi: 10.1111/gtc.12025
- Khosla, A., Morffy, N., Li, Q., Faure, L., Chang, S. H., Yao, J., et al. (2020). Structure-Function Analysis of SMAX1 Reveals Domains That Mediate Its Karrikin-Induced Proteolysis and Interaction with the Receptor KAI2. *Plant Cell* 32, 2639–2659. doi: 10.1105/tpc.19.00752
- Lee, H. W., Sharma, P., Janssen, B. J., Drummond, R. S. M., Luo, Z., Hamiaux, C., et al. (2020). Flexibility of the petunia strigolactone receptor DAD2 promotes its interaction with signaling partners. *J. Biol. Chem.* 295, 4181–4193. doi: 10.1074/jbc.RA119.011509
- Marzec, M., and Brewer, P. (2019). Binding or Hydrolysis? How Does the Strigolactone Receptor Work?. *Trends Plant Sci.* 24, 571–574. doi: 10.1016/j.tplants.2019.05.001
- Nakamura, H., Xue, Y. L., Miyakawa, T., Hou, F., Qin, H. M., Fukui, K., et al. (2013). Molecular mechanism of strigolactone perception by DWARF14. *Nat. Commun.* 4:2613. doi: 10.1038/ncomms3613
- Robert, X., and Gouet, P. (2014). Deciphering key features in protein structures with the new ENDscript server. *Nucleic Acids Res.* 42, W320–W324. doi: 10.1093/nar/gku316
- Sarrion-Perdigones, A., Vazquez-Vilar, M., Palaci, J., Castelijn, B., Forment, J., Ziarsolo, P., et al. (2013). GoldenBraid 2.0: a comprehensive DNA assembly framework for plant synthetic biology. *Plant Physiol.* 162, 1618–1631. doi: 10.1104/pp.113.217661
- Seto, Y., Yasui, R., Kameoka, H., Tamiru, M., Cao, M., Terauchi, R., et al. (2019). Strigolactone perception and deactivation by a hydrolase receptor DWARF14. *Nat. Commun.* 10:191. doi: 10.1038/s41467-018-08124-7

- Shabek, N., Ticchiarelli, F., Mao, H., Hinds, T. R., Leyser, O., and Zheng, N. (2018). Structural plasticity of D3-D14 ubiquitin ligase in strigolactone signalling. *Nature* 563, 652–656. doi: 10.1038/s41586-018-0743-5
- Sievers, F., Wilm, A., Dineen, D., Gibson, T. J., Karplus, K., Li, W., et al. (2011). Fast, scalable generation of high-quality protein multiple sequence alignments using Clustal Omega. *Mol. Syst. Biol.* 7:539. doi: 10.1038/msb.2011.75
- Song, X., Lu, Z., Yu, H., Shao, G., Xiong, J., Meng, X., et al. (2017). IPA1 functions as a downstream transcription factor repressed by D53 in strigolactone signaling in rice. *Cell Res.* 27, 1128–1141. doi: 10.1038/cr.2017.102
- Soundappan, I., Bennett, T., Morffy, N., Liang, Y., Stanga, J. P., Abbas, A., et al. (2015). SMAX1-LIKE/D53 Family Members Enable Distinct MAX2-Dependent Responses to Strigolactones and Karrikins in Arabidopsis. *Plant Cell* 27, 3143–3159. doi: 10.1105/tpc.15.00562
- Stanga, J. P., Smith, S. M., Briggs, W. R., and Nelson, D. C. (2013). SUPPRESSOR OF MORE AXILLARY GROWTH2 1 controls seed germination and seedling development in Arabidopsis. *Plant Physiol.* 163, 318–330. doi: 10.1104/pp.113.221259
- Stirnberg, P., Furner, I. J., and Ottoline Leyser, H. M. (2007). MAX2 participates in an SCF complex which acts locally at the node to suppress shoot branching. *Plant J.* 50, 80–94. doi: 10.1111/j.1365-313X.2007.03032.x
- Tena, E., Mekbib, F., and Ayana, A. (2016). Correlation and Path Coefficient Analyses in Sugarcane Genotypes of Ethiopia. *Am. J. Plant Sci.* 07, 1490–1497. doi: 10.4236/ajps.2016.710141
- Tuma, E. H. (1987). *Agricultural Innovation in the Early Islamic World: the Diffusion of Crops and Farming Techniques, 700–1100*. By Andrew M. Watson. Cambridge Studies in Islamic Civilization. New York: Cambridge University Press, 1983. 1983. Pp. x, 260. \$39.50. *J. Econ. Hist.* 47, 543–544. doi: 10.1017/s0022050700048531
- Umehara, M., Hanada, A., Yoshida, S., Akiyama, K., Arite, T., Takeda-Kamiya, N., et al. (2008). Inhibition of shoot branching by new terpenoid plant hormones. *Nature* 455, 195–200. doi: 10.1038/nature07272
- Wang, L., Wang, B., Jiang, L., Liu, X., Li, X., Lu, Z., et al. (2015). Strigolactone Signaling in Arabidopsis Regulates Shoot Development by Targeting D53-Like SMXL Repressor Proteins for Ubiquitination and Degradation. *Plant Cell* 27, 3128–3142. doi: 10.1105/tpc.15.00605
- Wang, L., Wang, B., Yu, H., Guo, H., Lin, T., Kou, L., et al. (2020). Transcriptional regulation of strigolactone signalling in Arabidopsis. *Nature* 583, 277–281. doi: 10.1038/s41586-020-2382-x
- Waters, M. T., Nelson, D. C., Scaffidi, A., Flematti, G. R., Sun, Y. K., Dixon, K. W., et al. (2012). Specialisation within the DWARF14 protein family confers distinct responses to karrikins and strigolactones in Arabidopsis. *Development* 139, 1285–1295. doi: 10.1242/dev.074567
- Yao, R., Ming, Z., Yan, L., Li, S., Wang, F., Ma, S., et al. (2016). DWARF14 is a non-canonical hormone receptor for strigolactone. *Nature* 536, 469–473. doi: 10.1038/nature19073
- Yao, R., Wang, L., Li, Y., Chen, L., Li, S., Du, X., et al. (2018). Rice DWARF14 acts as an unconventional hormone receptor for strigolactone. *J. Exp. Bot.* 69, 2355–2365. doi: 10.1093/jxb/ery014
- Zhang, J., Nagai, C., Yu, Q., Pan, Y.-B., Ayala-Silva, T., Schnell, R. J., et al. (2012). Genome size variation in three Saccharum species. *Euphytica* 185, 511–519. doi: 10.1007/s10681-012-0664-6
- Zhang, J., Zhang, X., Tang, H., Zhang, Q., Hua, X., Ma, X., et al. (2018). Allele-defined genome of the autopolyploid sugarcane *Saccharum spontaneum* L. *Nat. Genet.* 50, 1565–1573. doi: 10.1038/s41588-018-0237-2
- Zhao, L. H., Zhou, X. E., Wu, Z. S., Yi, W., Xu, Y., Li, S., et al. (2013). Crystal structures of two phytohormone signal-transducing alpha/beta hydrolases: karrikin-signaling KAI2 and strigolactone-signaling DWARF14. *Cell Res.* 23, 436–439. doi: 10.1038/cr.2013.19
- Zhou, F., Lin, Q., Zhu, L., Ren, Y., Zhou, K., Shabek, N., et al. (2013). D14-SCF(D3)-dependent degradation of D53 regulates strigolactone signalling. *Nature* 504, 406–410. doi: 10.1038/nature12878

Conflict of Interest: The authors declare that the research was conducted in the absence of any commercial or financial relationships that could be construed as a potential conflict of interest.

Publisher's Note: All claims expressed in this article are solely those of the authors and do not necessarily represent those of their affiliated organizations, or those of the publisher, the editors and the reviewers. Any product that may be evaluated in this article, or claim that may be made by its manufacturer, is not guaranteed or endorsed by the publisher.

Copyright © 2021 Hu, Zhao, Chen, Zhao, Wang, Feng, Wu, Xie, Zhou, Xiao, Ming, Zhang and Yao. This is an open-access article distributed under the terms of the Creative Commons Attribution License (CC BY). The use, distribution or reproduction in other forums is permitted, provided the original author(s) and the copyright owner(s) are credited and that the original publication in this journal is cited, in accordance with accepted academic practice. No use, distribution or reproduction is permitted which does not comply with these terms.